CONTROLLED LONGITUDINAL EMITTANCE BLOW-UP IN A DOUBLE HARMONIC RF SYSTEM AT CERN SPS

T. Argyropoulos, T. Bohl, T. Linnecar, E. Shaposhnikova, J. Tückmantel, CERN, Geneva, Switzerland

Abstract

Controlled longitudinal emittance blow-up together with a fourth harmonic RF system are two techniques that are being used in the SPS in order to stabilize the beam before injecting into the LHC. The emittance blow-up has been achieved by introducing a band-limited phase noise during acceleration. Measured variations of the final emittance along the batch can be explained by the modification of the synchrotron frequency distribution due to the effect of beam loading in a double harmonic RF system.

INTRODUCTION

The nominal LHC beam in the SPS consists of four batches separated by 3 gaps of 225 ns. Each batch contains 72 bunches spaced by 25 ns with 1.15×10^{11} protons per bunch. This beam is accelerated by four 200 MHz travelling wave cavities, equipped with feed-forward and feed-back systems. However, a longitudinal coupled bunch instability observed at high energies appeared to be a limiting factor because of its low threshold at 2×10^{10} p/b. This beam is finally stabilised by increased synchrotron frequency spread using a fourth harmonic RF system [1] and controlled longitudinal emittance blow-up which is applied during the ramp by introducing band limited noise through the phase loop of the main RF system [2].

Although the controlled emittance blow-up is necessary to stabilize the nominal intensity beam at flat top, the final bunch length and therefore emittance is limited due to the injection into the 400 MHz buckets of LHC. For that reason, bunch to bunch emittance variations along the batch can lead to particle losses in the LHC. Non-uniform emittance blow-up of high intensity beam in SPS had been observed at the end of 2004 and previous studies [3, 4] suggested that this effect can be attributed to the bunch to bunch variation of the incoherent synchrotron frequency due to the residual beam loading. This analysis showed that for the bunches at the edges of the batch the zero amplitude synchrotron frequency is lower than for those in the middle. Therefore, for a constant noise band along the batch for all bunches we would expect the blow-up to be more effective for those in the middle of the batch (optimum phasing). However, the experimental results show that bunches at the edges of the batch are blown-up more than those in the middle.

The present work extends the previous analysis by considering how the whole synchrotron frequency distribution is modified for the different bunches in the batch, defined mainly by the residual beam loading in the 200 MHz RF system. It will be shown that for the bunches at the edges of the batch, where the bigger synchronous phase variations due to beam loading occur, a significant change in the synchrotron frequency distribution appears, making larger blow-up possible.

OBSERVATION OF NON-UNIFORM EMITTANCE BLOW-UP

With the controlled emittance blow-up a stable beam of emittance up to ~0.6 eVs can be delivered to the LHC. However, the measurements that are presented here were done for a single batch with nominal intensity, with the aim to obtain maximum emittance (~0.9 eVs) for transfer to LHC which might be requested. Particle momentum and applied RF voltages (200 MHz and 800 MHz) for the SPS cycle are shown in Fig. 1. The band limited noise [2] was introduced through the phase loop of the 200 MHz RF system at 185 GeV (14.8 s along the cycle) and lasted for 3 s. Figure 2 depicts the noise band and the synchrotron frequency spread (calculated for low intensity) during the cycle where the noise is applied. For nominal intensity beam the low intensity settings should be shifted down by ~10 Hz due to an incoherent frequency shift produced by the SPS inductive impedance ImZ/n≃7 Ohm.

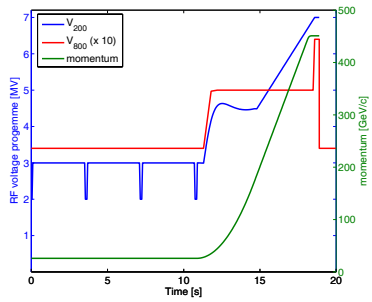

Figure 1: Particle momentum (green), the 200 MHz voltage (blue) and 800 MHz voltage (red, ×10) programme along the cycle.

The bunch lengths were deduced from the acquired bunch profiles after correcting for the pick-up and cable transfer function [5]. Figure 3 shows the results for two cycles where different noise bands were applied. The plots present the bunch lengths at different moments in the cycle. Both cases correspond to a successful blow-up in the sense that at the flat top the bunches were stable. However, it is apparent that bigger blow-up occurs for the bunches at the beginning and the end of the batch. Furthermore, we can clearly see from the bottom plot where the noise band was lifted up 10 Hz compared to the top one, that the relative

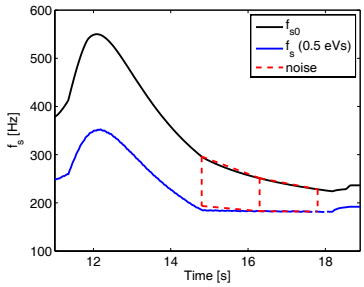

Figure 2: Noise excitation (red dashed lines) and synchrotron frequency spread at the end of the cycle, calculated for low intensities and for a bunch of 0.5 eVs.

excitation of the bunches in the edges of the batch was less compared to those in the middle.

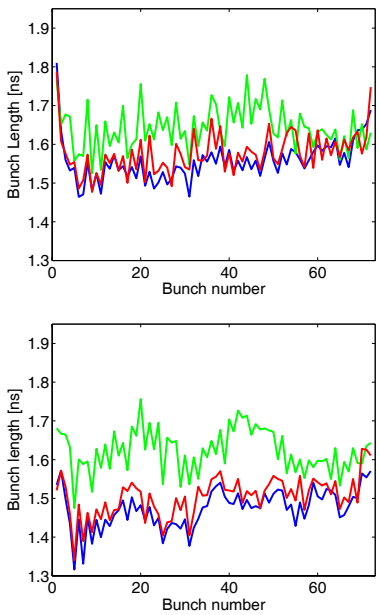

Figure 3: Measured bunch lengths before the blow-up (green), just after (red) and at the flat top of the cycle (blue). The noise frequency band was shifted down ~20 Hz (275-175 Hz) at the top plot and ~10 Hz (285-185 Hz) at the bottom with respect to the calculated values (low intensity).

The bunch position variation along the batch Δt (found from the bunch profiles after a Gaussian fit), which corresponds in the stable situation to the synchronous phase displacement $\Delta\phi_s = \omega_{rf}\Delta t$ (ω_{rf} is the 200 MHz RF frequency), is shown in Fig. 4 for the same data presented in Fig. 3. The antisymmetric pattern of the curves before the noise excitation (green line) indicates that the bunch positions are mainly defined by the beam loading in the main 200 MHz RF system, compensated by the feed-back and feed-forward systems. At flat top (blue line), where the bunch lengths become smaller the effect of the 800 MHz beam loading, without feed-back and feed-forward systems, also becomes non negligible and it disturbs the previous pattern. The effects of beam loading are considered in the next section.

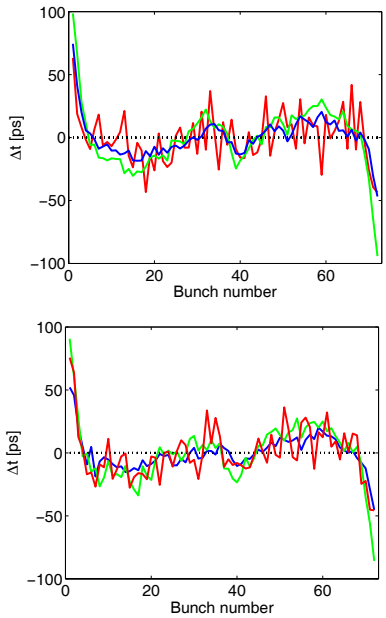

Figure 4: Longitudinal bunch position shift with respect to nominal position along the batch. The data correspond to those of Fig. 3.

BEAM LOADING EFFECTS

It is apparent from the measurements presented in the previous section that the beam loading in the RF cavities of the SPS, for nominal intensity beam, is changing significantly the position of the bunches along the batch. For this reason the calculation of the beam loading effects is presented in this section, based on the theory of the travelling wave RF systems given in [6].

The DC beam current for bunches with 25 ns bunch spacing and 1.15×10^{11} protons per bunch is 0.74 A. For a Gaussian distribution, the 200 MHz fourier component of the beam current would be around 1.30 A before the blow up (bunch lengths~1.7 ns), while the 800 MHz component would be about 0.15 A. The induced accelerating voltage V_b in the cavity depends on the filling time τ_f. When the batch enters the cavity the bunches at the head see only the accelerating voltage created by the power amplifiers V_{rf}. As more bunches enter the cavity the induced voltage finally reaches a steady value according to the filling time of the cavity. The first situation is defined as transient beam loading state, while the second is called steady state.

The beam loading impedance $Z_b = \frac{V_b}{I_b}$ defined from the ratio between the beam induced voltage V_b and the beam current I_b is given, for a travelling wave cavity, by the formula [6]

$$Z_b = -\frac{L^2 R_2}{8}\left[\left(\frac{\sin\frac{\tau}{2}}{\frac{\tau}{2}}\right)^2 - j\cdot 2\frac{\tau-\sin\tau}{\tau^2}\right], \qquad (1)$$

where R_2 is the series impedance of the travelling wave cavity, L the interaction length and τ the total phase slip

between the proton bunches and the travelling wave, given as a function of the RF frequency ω by

$$\tau = \frac{L}{v_g}(\omega - \omega_0), \tag{2}$$

where ω_0 is the cavity central frequency, v_g is the group velocity, given in the travelling wave cavity by $v_g/c = 0.0946$. The parameters of the cavities that were used for the calculations of the impedances are listed in Table 1.

In the case of the 200 MHz RF system the 4 travelling wave cavities (2 short and 2 long) are equipped with a feed-forward and a one turn feed-back system which compensate the beam loading effect [7, 8] by modifying the impedance Z_b. For the 800 MHz RF system two travelling wave cavities are installed but only one is used for acceleration, without feed-back or feed-forward systems (to be installed in 2011). Figure 5 presents the calculated values of the induced voltage in the 200 MHz (feed-forward and feed-back were taken into account) and 800 MHz RF systems just before the noise application.

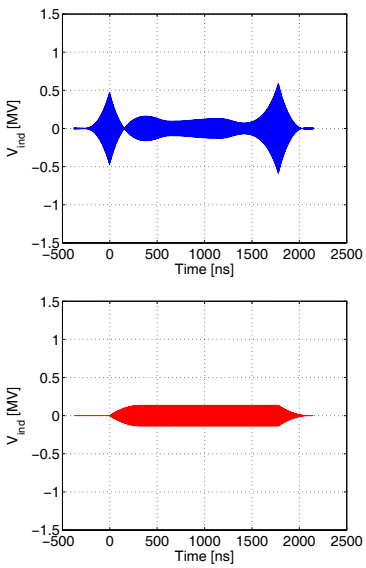

Figure 5: Calculated beam induced voltage in the 200 MHz (top) and 800 MHz (bottom) RF systems just before the noise excitation. $V_{200} = 4.5$ MV and $V_{800} = 0.5$ MV. The time 0 is when the first bunch enters the cavity.

The total voltage V_t seen by a synchronous particle passing through a travelling wave cavity (200 MHz or 800 MHz) is given by

$$\vec{V}_t = \vec{V}_{rf} + \vec{V}_b \tag{3}$$

This equation for the steady state value of V_b (in the centre of the batch) is visualized in the case of acceleration, in the top vector diagram of Fig. 6 (black arrows). With respect to the beam current I_b, the accelerating voltage of the power amplifier V_{rf} is placed at angle ϕ_L, while the beam induced voltage V_b is at angle -τ/3. This angle is calculated from the beam loading impedance and is defined as the beam loading angle. The angle ϕ_s corresponds to the synchronous phase.

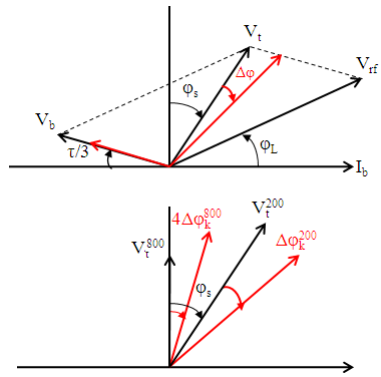

Figure 6: Vector diagram showing the beam loading voltage. On top for one cavity at steady (black) and transient (red) state and on bottom for both the 200 MHz and 800 MHz RF systems.

From the vector diagram the following relations can be obtained

$$\tan\phi_L = \frac{V_t\cos\phi_s - V_b\sin\tau/3}{V_t\sin\phi_s + V_b\cos\tau/3} \tag{4}$$

$$V_{rf} = \frac{V_t\sin\phi_s + V_b\cos\tau/3}{\cos\phi_L} \tag{5}$$

For fixed V_{rf} in the top vector diagram the variation of the synchronous phase $\Delta\phi_k$ (bunch position) according to the values of the induced voltage V_{bk} along the batch (red arrows in Figure 6) can be calculated.

$$\tan(\phi_s + \Delta\phi_k) = \frac{V_{rf}\cos\phi_L - V_{bk}\cos\tau/3}{V_{rf}\sin\phi_L + V_{bk}\sin\tau/3}, \tag{6}$$

where k corresponds to the bunch number along the batch. The formalism described above can be used to calculate the phase shift along the batch for the 200 MHz ($\Delta\phi_k^{200}$) and the 800 MHz ($\Delta\phi_k^{800}$) RF systems with the only difference that in the case of 800 MHz RF system the phase ϕ_s in the top vector diagram of Fig. 6 is 0. The phase shift variations $\Delta\phi_k^{200}$ and $\Delta\phi_k^{800}$ of the two RF systems can be used in order to find the total phase shift, by taking into account that the vectors V_t^{200} and V_t^{800} found for each RF system have a phase angle ϕ_s for the steady state (black arrows at bottom plot of Fig. 6). Note that here is considered only the case where phasing between the two RF systems is established using measurements in the middle of the batch. According to that the phase shift $\Delta\phi_{sk}$ can be derived from

$$\tan(\Phi_{sk}) = \frac{V_{tk}^{200}\sin(\Phi_k^{200}) + V_{tk}^{800}\sin(\Delta\phi_k^{800})}{V_{tk}^{200}\cos(\Phi_k^{200}) + V_{tk}^{800}\cos(\Delta\phi_k^{800})} \tag{7}$$

where $\Phi_{sk} = \phi_{s0} + \Delta\phi_{sk}$, ϕ_{s0} is the synchronous phase of the total voltage for the steady state and $\Phi_k^{200} = \phi_s + \Delta\phi_k^{200}$.

Table 1: Parameters of the Travelling Wave Cavities (2 of each Type)

	200 MHz Long	200 MHz Short	800 MHz
Centre frequency	200.222 MHz	200.222 MHz	800.888 MHz
Interaction length	20.196 m	16.11 m	3.46 m
Series impedance R_2	27.1 kΩ/m^2	27.1 kΩ/m^2	647 kΩ/m^2
Filling time L/v_g	0.712 µs	0.568 µs	0.330 µs
Beam loading impedance $L^2R_2/8$	1.38 MΩ	0.879 MΩ	0.968 MΩ

Calculation of the Bunch Position

Using Eq. (7) we can calculate the variation of the synchronous phase $\Delta\phi_{sk}$ which corresponds to the bunch position variation along the batch, just before the noise excitation. The results for both 200 MHz and 800 MHz RF systems are plotted in Fig. 7 (solid line). An example of measured bunch positions is also presented for comparison (dashed line).

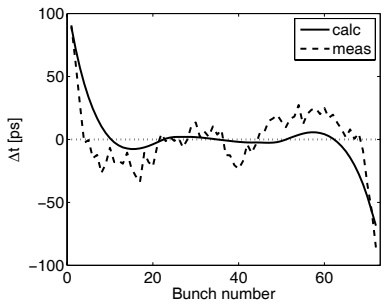

Figure 7: Bunch position variation along the batch at the time in the cycle before the noise excitation. V_{200} = 4.5 MV and V_{800} = 0.5 MV.

We can clearly see that our model can closely reproduce the measurements, indicating that the main cause of the bunch position variation is the induced voltage in the RF systems. However, the difference shows that there are other parameters that have not been taken into account in the consideration of the model.

The total external voltage that is seen by the particle in the centre of the batch, considering both V_{rf} and V_b for the two RF systems is

$$V = V_t^{200}\sin\phi + V_t^{800}\sin(4\phi + \Phi_2) \tag{8}$$

where Φ_2 is programmed to $\Phi_2 = -4\phi_s + \pi$ for the bunch shortening mode above transition. The induced voltage in the 200 MHz system is changing the bunch position by $\Delta\phi_{sk}$. Taking into account that the phase shift between the 200 MHz and 800 MHz RF systems is fixed at ϕ_s for $\Delta\phi_{sk} = 0$ (Fig. 6), this change of synchronous phase due to beam loading in 200 MHz is equivalently introduced in Φ_2.

$$V = V_t^{200}\sin\phi + V_t^{800}\sin(4\phi + \Phi_2 + \Delta\phi_2), \tag{9}$$

where $\Delta\phi_2 = 4\Delta\phi_s$. Due to the presence of the second RF system the synchronous phase changes by an angle $\delta\phi_s$. Considering now that the measured shift of the bunch positions $\Delta\phi_s^{meas}$ is given by the sum

$$\Delta\phi_s^{meas} = \Delta\phi_s + \delta\phi_s \tag{10}$$

we can estimate that

$$\delta\phi_s = \frac{V_t^{800}\sin(4\Delta\phi_s^{meas})}{V_t^{200}\cos\phi_s}. \tag{11}$$

From Eqs. (10) and (11) we have

$$\Delta\phi_2 = 4\left(\Delta\phi_s^{meas} - \frac{V_t^{800}\sin(4\Delta\phi_s^{meas})}{V_t^{200}\cos\phi_s}\right), \tag{12}$$

which for small values of $\Delta\phi_s^{meas}$ can be simplified to

$$\Delta\phi_2 = 4\Delta\phi_s^{meas}\left(1 + 4\frac{V_t^{800}}{V_t^{200}(-\cos\phi_s)}\right) \tag{13}$$

This means that for the batch edges, where $\Delta t_{meas} \simeq 100\ ps$ we have $\Delta\phi_2 \simeq 40°$. Inserting this value into (9) we can calculate the synchrotron frequency distribution inside the bunch using for Φ_2 the programmed value. The results are plotted in Fig. 8 for $\Delta\phi_2 = 0, \pm 40°, \pm 70°$. In the plot the noise frequency bands were lifted up by 10 Hz (195-295 Hz and 185-285 Hz) compared to those used in operation (185-285 Hz and 175-275 Hz), since for the calculations the synchrotron frequency shift due to the SPS inductive impedance was not taken into account .

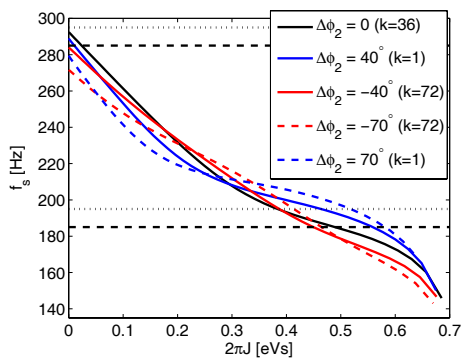

Figure 8: Synchrotron frequency distribution as a function of action normalized to emittance calculated for the voltage of Eq. (9) with $\Phi_2 = -4\phi_s + \pi$. The dotted and dashed lines present the phase noise bands that were used.

The blue curve in Fig. 8 shows that for one end of the batch (k=1), a flat region ($\omega'(J) \sim 0$) appears on the synchrotron frequency distribution, indicating that these bunches for fixed noise band can be blown-up more (0.57 eVs, 0.59 eVs) than those at the centre of the batch (k=36, 0.49 eVs). On the other hand, the synchrotron frequency distribution is different for the opposite batch end (k=72, red curve) which shows that this bunch is blown-up less (0.45 eVs, 0.465 eVs). The system is very sensitive to the differences in Φ_2 and since the calibration of the phase shift between the two RF systems is based on beam measurements (bunch shape or beam stability) [4] we always have an offset which in general is not known. For that reason the synchrotron frequency distribution can be significantly modified. In addition the calculated value of Φ_2 [1] is different from the programmed one by $\sim 10^\circ$ at 800 MHz. Of course the difference is not big but larger variation can cause critical changes in the synchrotron frequency distributions.

In addition to the bunch to bunch offset in Φ_2 the total voltage is also different for the bunches at the edges of the batch, because of beam loading. Figure 9 shows the synchrotron frequency distribution after taking into account the voltage modulation at the edges of the batch (k=1 and k=72). For Φ_2 the programmed value was used, while a larger value of $\Delta\phi_2 = \pm 70^\circ$ was used, in order to demonstrate the sensitivity of the synchrotron frequency distribution for this parameter.

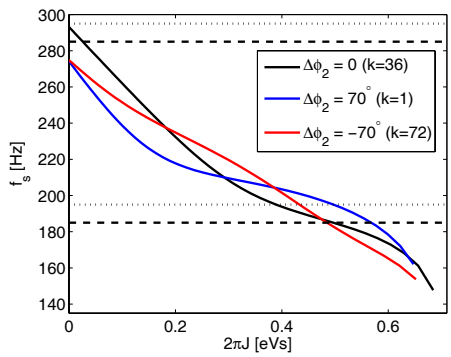

Figure 9: Synchrotron frequency distribution as a function of emittance. The change in the total voltages at the edges of the batch was taken into account. Same color code as in Fig. 8.

The last plot gives an example where the bunches for the extreme cases of $\Delta\phi_2$ are more blown-up for the applied noise bands. This difference becomes more pronounced during the 3 seconds of the noise excitation where the bunch parameters are changing. For a more accurate model we need to implement also the potential well distortion that occurs from other impedances and in particular the kickers. This impedance does not introduce a difference from bunch to bunch but still modifies the synchrotron frequency distribution. Furthermore, locking the phase of the voltage in the two RF systems by a measurement outside the batch can also affect significantly the results.

CONCLUSIONS

Controlled longitudinal emittance blow-up together with the operation of a high harmonic RF system are essential for the LHC beam stabilization in the SPS. Measurements of bunch lengths at the flat top show that after the noise excitation a non-uniform emittance blow-up occurs. Taking into account the residual beam loading in the 200 MHz RF system and the beam induced voltage in the 800 MHz RF system the observed variation of the bunch position along the batch can be closely reproduced. The bunch positions are mainly modified by the residual beam loading in the 200 MHz RF system. The synchrotron frequency distribution calculated for bunches at different positions in the batch using the total voltage derived from this model can explain the large variation in emittance along the batch for the applied phase noise band.

We would like to thank G. Papotti for her help during the measurements.

REFERENCES

[1] T. Bohl, T. Linnecar, E. Shaposhnikova, J. Tückmantel, “Study of Different Operating Modes of the 4th RF Harmonic Landau Damping System in the CERN SPS”, EPAC’98, Stockholm, Sweden, 1998.

[2] J. Tückmantel, “Digital Generation of Noise-Signals with Arbitrary Constant or Time-Varying Spectra”, CERN-LHC-PROJECT-Report-1055 (February 2008).

[3] E. Shaposhnikova, “Cures For Beam Instabilities in the CERN SPS and their Limitations”, Proc. of HB2006, Tsukuba, Japan, 2006.

[4] G. Papotti, T. Bohl, T. Linnecar, E. Shaposhnikova, J. Tückmantel, “Study of Controlled Longitudinal Emittance Blow-up for High Intensity LHC Beams in the CERN SPS”, Proc. of EPAC’08, Genoa, Italy, 2008.

[5] T. Bohl, “Bunch length measurements with the SPS AEW.31731 wall current monitor”, AB Note 2007-032 (RF) (June 2007).

[6] G. Dôme, “The SPS Acceleration System / Travelling Wave Drift-Tube Structure for the CERN SPS”, CERN-SPS-ARF-77-11 (May 1977).

[7] D. Boussard, “Beam Loading”, CERN Accelerator School, Oxford, England, 16-27 September 1985, CERN 87-03, 21 April 87.

[8] P. Baudrenghien, G. Lambert, “Control of strong beam loading Results with beam”, 11th Workshop of the LHC, 15 - 19 Jan. 2001, Chamonix, France, CERN-SL-2001-003.